Barrier to Methyl Internal Rotation of Cis- and *Trans*-2-Methylvinoxy Radicals in the $\tilde{X}(^2A'')$ and $\tilde{B}(^2A'')$ States: Experiment and Theory

Sarah Williams,[†] Lawrence B. Harding,[‡] John F. Stanton,[§] and James C. Weisshaar*[,†]

Department of Chemistry, University of Wisconsin-Madison, Madison, Wisconsin 53706-1396, Chemistry Division, Argonne National Laboratory, Argonne, Illinois 60439, and Institute of Theoretical Chemistry, Department of Chemistry and Biochemistry, University of Texas at Austin, Austin, Texas 78712

Received: July 7, 2000; In Final Form: August 22, 2000

The jet-cooled laser induced fluorescence spectrum of the $\tilde{B} \leftarrow \tilde{X}$ electronic transition of 2-methylvinoxy radical is assigned as a superposition of contributions from noninteracting cis and trans isomers. The spectrum of the cis isomer is identified by comparison with ab initio electronic structure calculations; both theory and experiment clearly indicate that the methyl conformation changes from the $\tilde{X}$ state to the $\tilde{B}$ state. Fits of both hot and cold bands to a one-dimensional torsional model yield methyl rotor barrier magnitudes of 270 ± 20 cm^{-1} in the $\tilde{X}$ state and 200 ± 20 cm^{-1} in the $\tilde{B}$ state. The ab initio calculations show that in the ground state the preferred conformation places one methyl CH bond in the plane of the molecular frame cis to the vicinal CC bond. Assignment of the spectrum of *trans*-2-methylvinoxy is more tentative because no resolved hot bands are available to corroborate the model. Our best estimate for the $\tilde{B}$ state barrier magnitude is 60 ± 15 cm^{-1}. Multireference configuration interaction calculations and coupled cluster calculations are reasonably successful in obtaining methyl torsional barriers in agreement with experiment, although high accuracy is elusive for the $\tilde{B}$ state of both cis and trans isomers. By comparison with simpler cases, we infer that the π radical character of the $\tilde{B}$ state strongly influences the methyl torsional barrier.

I. Introduction

Vinoxy radicals are important reactive intermediates in both combustion and atmospheric chemistry. In particular, methyl-substituted vinoxy radicals are primary products of the combustion reactions of $O(^3P)$ with various alkenes.[1−3] In atmospheric chemistry, vinoxy radicals are likely important intermediates in the reactions of ozone with alkenes, eventually contributing significantly to the generation of HO_x radicals in the troposphere.[4] In addition, understanding the behavior of methyl rotors adjacent to a radical center is of fundamental interest in mechanistic organic chemistry. Finally, in large molecules methyl rotors enhance the density of rovibrational states, which in turn governs the rate of intramolecular vibrational energy redistribution (IVR).[5−8]

We recently presented a detailed study of the spectroscopy of the 1-methylvinoxy radical,[9] including assignment of the $\tilde{B} \leftarrow \tilde{X}$ laser-induced fluorescence (LIF) spectrum. The cold band structure near the $\tilde{B}$-state origin yields the magnitude of the barrier to internal methyl rotation in the upper electronic state. Hot bands yield the same for the ground state. The intensities of the band within the torsional envelope clearly show that the methyl group undergoes a change in conformational preference upon $\tilde{B} \leftarrow \tilde{X}$ excitation. With help from extensive electronic structure calculations, we concluded that the preferred 1-methylvinoxy conformation places one methyl CH bond cis to the CO bond in the $\tilde{X}$ state (130 ± 30 cm^{-1} barrier height) but trans to the CO bond in the $\tilde{B}$ state (740 ± 30 cm^{-1} barrier height).

In this paper, we assign and analyze the cis and *trans*-2-methylvinoxy $\tilde{B} \leftarrow \tilde{X}$ LIF spectrum. For the cis isomer, both $\tilde{X}$ and $\tilde{B}$-state methyl rotor barriers are experimentally determined from assignment of hot and cold bands as described above. Like 1-methylvinoxy, *cis*-2-methylvinoxy undergoes a change in preferred methyl conformation upon excitation. Electronic structure calculations determine that the preferred conformations places one methyl CH bond in the plane of the radical cis to the vicinal C_1C_2 bond in the $\tilde{X}$ state (Figure 1) and trans to the C_1C_2 bond in the $\tilde{B}$ state. The experimentally determined barrier heights for the cis isomer are 200 ± 40 cm^{-1} and 268 ± 40 cm^{-1}, respectively.

For the trans isomer, due to lack of assigned hot bands, only the $\tilde{B}$-state methyl torsional barrier of 60 ± 15 cm^{-1} is experimentally determined. The experimental intensity pattern and electronic structure calculations both indicate that *trans*-2-methylvinoxy radical does not change its preferred methyl conformational preference upon excitation. The computational work determines that the preferred methyl group conformation in both $\tilde{X}$ and $\tilde{B}$ states places one methyl CH bond cis to the C_1C_2 vicinal bond.

A series of detailed ab initio electronic structure calculations were performed on the ground and $\tilde{B}$ excited state of both 2-methylvinoxy isomers. These included complete active space self-consistent field (CASSCF) calculations, multireference configuration interaction (CAS+1+2) calculations, and coupled-cluster (CC) calculations. In the previous work on 1-methylvinoxy,[9] calculations that reproduce experimental $\tilde{B} \leftarrow \tilde{X}$ electronic transition energies and $\tilde{B}$-state vibrational frequencies quite well struggled to adequately predict the methyl rotor barrier. The CC calculations with largest basis set were most successful. In the case of 2-methylvinoxy isomers, CAS+1+2 and CC methods are comparably successful in determining the

[†] Department of Chemistry, University of Wisconsin−Madison.
[‡] Chemistry Division, Argonne National Laboratory.
[§] Institute of Theoretical Chemistry, Department of Chemistry and Biochemistry, University of Texas at Austin.

10.1021/jp002431+ CCC: $19.00 © 2000 American Chemical Society
Published on Web 10/13/2000

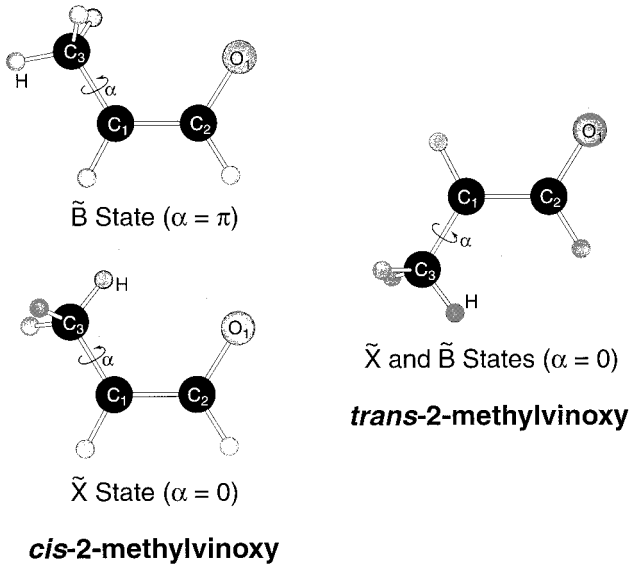

Figure 1. Methyl rotor conformations of minimum energy for cis and *trans*-2-methylvinoxy radical in both $\tilde{X}$ and $\tilde{B}$ electronic states, based on a combination of experiment and theory. Atomic labeling scheme for ab initio calculations as shown. Methyl torsional angle α defined as the dihedral angle $H-C_3-C_1-C_2$ for both cis and trans isomers.

methyl rotor barriers, but the $\tilde{B}$-state barriers remain difficult to compute to high accuracy.

II. Experiment

The experimental apparatus has been described in detail elsewhere.[10] Briefly, the 2-methylvinoxy radicals are prepared by 193 nm photolysis of a mixture of *cis*- and *trans*-ethyl-2-propenyl ether, $CHCH_3{=}CHOCH_2CH_3$, at the nozzle of a pulsed jet expansion of 2−3 atm Ar through a 1 mm diameter nozzle. The radicals are probed 7 cm downstream with a frequency doubled Nd:YAG pumped dye laser near 345 nm (pulse width 10 ns fwhm, bandwidth 0.2 cm^{-1} fwhm, typical pulse energy 2 mJ/pulse). A photomultiplier tube perpendicular to both the probe laser and the axis of the pulsed jet detects the resulting fluorescence. The resulting LIF spectra have not been normalized to laser power, which varies roughly ±20% over the frequency range of interest, 29,000−30,300 cm^{-1}. Band positions are measured as the intensity maxima; reported absolute frequencies are accurate to ±2 cm^{-1}. The narrowest bands are 4.5 cm^{-1} fwhm with differences in band frequencies accurate to ±0.6 cm^{-1}.

We attempted to distinguish the spectrum of *cis*-2-methylvinoxy from *trans*-2-methylvinoxy as follows. The precursor arrives as a mixture of approximately 65% cis and 35% trans isomers, as judged by NMR spectral intensities for the neat liquid. Because the cis precursor boils at 69 °C, whereas the trans precursor boils at 75 °C, we were able to partially separate the precursor isomers by distillation. We could create mixtures that varied in cis:trans composition by a factor of 16, from 4:1 to 1:4 as determined by NMR spectra. Moreover, these precursor mixtures were stable on the time scale of our experiment, indicating a large barrier to *cis*−*trans* interconversion in the precursor compound. However, within experimental uncertainty, both mixtures produced the same LIF spectrum shown in Figure 2. Evidently, we always obtained the LIF spectrum of the *same* mixture of cis and *trans*-2-methylvinoxy. It appears that under our photolysis conditions, the cis-trans isomerization of the radical photoproducts is rapid on the time scale of expansion and cooling. This probably results from the large internal energy

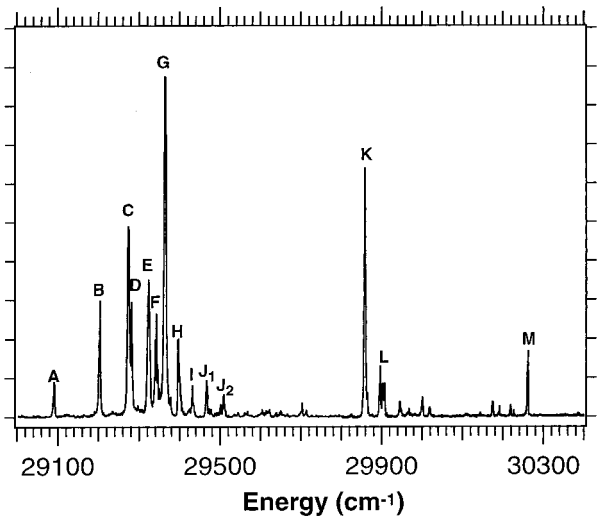

Figure 2. $\tilde{B} \leftarrow \tilde{X}$ LIF spectrum of a mixture of cis and *trans*-2-methylvinoxy radicals.

deposited in the nascent radicals. Computational results (discussed below) indicate a cis-trans isomerization barrier on the order of 10 kcal/mol in both the $\tilde{X}$ and $\tilde{B}$ states of 2-methylvinoxy.

The degree of vibrational cooling of the radicals can be coarsely adjusted by using a 1 m convex spherical lens to focus the photolysis laser to a 5 mm × 2 mm spot as it meets the gas pulse. Hot bands can thus be distinguished from cold bands. The coldest spectra are used to probe the methyl torsional potential of the $\tilde{B}$ state, while the hot bands from warmer spectra provide analogous information about the $\tilde{X}$ state.

III. Spectroscopic Background

A. Selection Rules. The well-studied $\tilde{B} \leftarrow \tilde{X}$ electronic spectrum of the vinoxy radical itself, as well as its fluoro- and methyl-substituted analogues, are examples of $\pi^* \leftarrow \pi$ transitions with both states of $^2A''$ symmetry.[10−13] In the 2-methylvinoxies, placing a methyl CH bond in the plane of the molecule allows classification under the C_s point group. Because the methyl torsional motion is feasible on experimental time scales, the internal symmetry is higher than that of the point-group symmetry. The molecular Hamiltonian can thus be defined in a symmetry allowing for all energetically feasible permutations and permutation-inversions of equivalent nuclei.[14,15] For the 2-methylvinoxies the molecular states are classified according to the irreducible representations of the molecular symmetry group G_6, which is isomorphic to the C_{3v} molecular point group.

Under G_6, the $\tilde{B} \leftarrow \tilde{X}$ electronic transition is $A_1 \leftarrow A_1$. Translations along the principal axes *a*, *b*, and *c* transform as a_1, a_1, and a_2, respectively. The $\tilde{B} \leftarrow \tilde{X}$ electronic transition is therefore allowed and polarized in the plane of the vinoxy skeleton, resulting in type AB hybrid bands. The appropriate symmetry labels for the pure torsional levels of 1-methylvinoxy are a_1, a_2, and *e*. As is customary, we label each stack of torsional states $0a_1$, $1e$, $2e$, $3a_2$, $3a_1$, $4e$, $5e$, $6a_2$, $6a_1$, and $7e$ in order of increasing torsional energy. The Franck−Condon allowed pure torsional transitions then follow the selection rules: $a_1 \leftrightarrow a_1$, $a_2 \leftrightarrow a_2$, and $e \leftrightarrow e$. These should be the strongest bands observed near the $\tilde{B}$-state origin. At higher energy in the $\tilde{B}$-state, we expect mixing of pure torsional states with low-frequency vibrational states and with torsion-vibration combination states as well as the onset of new Franck−Condon active vibrations and their associated torsional states. The spectral complexity can thus increase dramatically with $\tilde{B}$ state energy.

On the basis of experience with similar systems,[16−18] the conditions of the expansion in our experiment should effectively relax the 300 K torsional population distributions to the lowest spin allowed level, i.e., $0a_1$ for all *a*-symmetry and $1e$ for all *e*-symmetry levels. By conservation of nuclear spin symmetry the *a* and *e* levels do not interconvert. In this limit, the singly degenerate *a* torsional levels and the doubly degenerate *e* torsional levels of the methyl group have equal nuclear spin statistical weight factors.

B. Torsional States and Spectral Fitting. To solve the hindered internal rotation problem, we treat the methyl group and molecular frame as rigid rotors. Neglecting overall rotation and torsion-rotation coupling, the torsional Hamiltonian can be written in its simplest form[19]

$$H(\alpha) = -Fp^2 + V(\alpha) \tag{1}$$

where F is the reduced rotational constant for the methyl group relative to the HCCHO molecular frame, α is the torsional angle as referenced to the frame, and p is the torsional angular momentum conjugate to α. We define $\alpha = 0$ as the conformation with one methyl CH bond in the plane of the molecular frame cis to the vicinal C_1C_2 bond. Because the methyl rotor top axis does not coincide with any of the principal axes of the molecule, F is given by $1/2rI_\alpha$. Here I_α is the moment of inertia of the $-CH_3$ top about its symmetry axis and $r = 1 - I_\alpha(\lambda_a^2/I_a + \lambda_b^2/I_b + \lambda_c^2/I_c)$, where I_a, I_b, and I_c are the principal moments of inertia for the entire molecule including the methyl group and λ_a, λ_b, and λ_c are the direction cosines between the inertial axes and the methyl top axis of rotation. $V(\alpha)$ is the one-dimensional torsional potential modeled by using the conventional symmetry-adapted Fourier expansion

$$V(\alpha) = \sum_n \frac{V_{3n}}{2}(1 - \cos 3n\alpha),\ n = 0, 1, 2, \ldots \tag{2}$$

Because this expansion converges rapidly, it is generally appropriate to neglect terms higher than $n = 2$.

For the $\tilde{B}$ and $\tilde{X}$ states of *cis*-2-methylvinoxy and for the $\tilde{B}$ state of *trans*-2-methylvinoxy, the data will allow us to determine a 3-fold term V_3 and a small 6-fold term V_6. In each case, $|V_3|$ gives the magnitude of the barrier to internal rotation. For $V_6 \ll V_3$, the small 6-fold term controls the width of the barrier. The sign of V_3 fixes the lowest energy conformation. With our choice of $\alpha = 0$, for $V_3 > 0$, the potential minima lie at $\alpha = 0°$, 120°, and 240° in what we call the cis conformation. For $V_3 < 0$, the potential minima occur at $\alpha = 60°$, 180°, and 300°, the trans conformation. Unlike pure 6-fold cases where the torsional barriers are very small, the 3-fold barriers typically encountered localize probability density for the lowest levels in the potential wells. In the limit of a large barrier, pairs of *a* and *e* levels converge in energy to become 3-fold degenerate vibrational levels as follows: $0a_1$ and $1e \rightarrow v = 0$; $2e$ and $3a_2 \rightarrow v = 1$; $3a_1$ and $4e \rightarrow v = 2$; and so forth.

To model the spectra, we diagonalize the Hamiltonian in a basis set of 80 free rotor eigenfunctions ($e^{im\phi}$, $m = 0, \pm1, \pm2, \ldots$) as before.[20] The matrix elements are

$$H_{m,m'} = Fm^2\delta_{m,m'}$$

$$Hm,m'\pm3 = -\frac{V3}{4}\delta m,m'\pm3$$

$$H_{m,m'\pm6} = -\frac{V_6}{4}\delta_{m,m'\pm6} \tag{3}$$

We first determine the best $\tilde{B}$-state parameters from the vibrationally cold spectrum with V_3'' fixed at either the experimentally or, lacking that, the theoretically determined $\tilde{X}$-state barrier height as described below. This fitting procedure is not very sensitive to the choice of $\tilde{X}$-state parameters as long as V_3'' is larger than about 100 cm^{-1} and the proper change in the potential minimum from $\tilde{X}$ to $\tilde{B}$ is included. In the case of the cis isomer, we freeze V_3' and V_6' at the best values and then determine V_3'' from the hot bands measured in the vibrationally hot spectrum.

IV. Experimental Results and Discussion

A. Cold Bands. The $\tilde{B} \leftarrow \tilde{X}$ LIF spectrum of the cis and *trans*-2-methylvinoxy radicals (Figure 2) spans the range from 29 090−30 260 cm^{-1} and consists of over twenty vibronic bands. A detailed list of band frequencies was given earlier.[10] In comparison, the $\tilde{B} \leftarrow \tilde{X}$ LIF spectrum of the unsubstituted vinoxy radical consists of about seven strong bands spanning the range 28 785−30 200 cm^{-1}, whereas that of 1-methylvinoxy radical consists of over fifty vibronic bands spanning the range of 27 282−30 000 cm^{-1}.[9] All three LIF spectra die off at higher energy due to rapidly decreasing lifetimes.[10,11,21]

Although at first the 2-methylvinoxy spectrum might appear easier to assign than the more congested 1-methylvinoxy,[9] our 2-methylvinoxy assignments are in fact more tentative. The difficulties in assigning the 2-methylvinoxy spectrum are 2-fold. The first complication is that it represents a mixture of two radical isomers. Ab initio calculations described below indicate that the isomerization barrier to *cis*−*trans* isomerization is greater than 7 kcal/mol in both $\tilde{X}$ and $\tilde{B}$ states. On the basis of these calculations and the invariance of the spectrum to the mixture of radical precursor, the spectrum likely represents vertical excitation from two distinct, noninteracting isomers in the ground state to two distinct, noninteracting isomers in the $\tilde{B}$ state. In that case, the one-dimensional torsional model of Section III should work well at least at low internal energy in each isomer. The second difficulty in assigning the spectrum is that it lacks the expected repeating pattern of low-frequency torsional transitions that one expects from the well-studied $\tilde{B} \leftarrow \tilde{X}$ geometry changes in plain vinoxy. Assuming that the methyl rotor potential is approximately independent of vibrational state, every vibrational transition should repeat a particular torsional envelope as a series of combination bands of vibrational and torsional mode quanta. Such repeated torsional envelopes were indeed observed in 1-methylvinoxy, but they are not present in 2-methylvinoxy. The photochemical implications of this result are discussed briefly below.

We are able to assign one progression in the spectrum to each isomer. First, the *A*−*B*−*C*−*D*−*E* series was fit to the one-dimensional torsional model and securely assigned to the *cis*-2-methylvinoxy radical. This assignment (Table 1) is based on the fact that the intensity envelope clearly shows that the methyl rotor has changed its preferred conformation between the $\tilde{X}$ and $\tilde{B}$ states. Ab initio calculations (Section V) on the cis and *trans*-2-methylvinoxy radicals indicate that the cis isomer changes its preferred conformation upon excitation, whereas the trans isomer does not. Theory has successfully determined these conformational changes in previous studies of 1-methylvinoxy[9] and of substituted toluenes.[20,22] The hot band assignments described below will corroborate this scheme.

We fit both the frequencies and intensities of the *A*−*B*−*C*−*D*−*E* pattern of bands to the one-dimensional torsional Hamiltonian of eqs 2 and 3. Our fitting procedure includes three adjustable parameters for the $\tilde{B}$ state: F', V_3', and V_6'. The $\tilde{X}$-

TABLE 1: *Cis*-2-methylvinoxy $\tilde{B}$-state Assignments

band	assign	energy[a] (cm^{-1})	$\tilde{B}$−state expt.[b]	$\tilde{B}$−state calcd[c]	intensity expt[b]	intensity calcd[c]
A	$m_{0a_1}^{0a_1}, m_{1e}^{1e}$	29 090.1	0	0	0.2	0.03
B	m_{1e}^{2e}	29 202.5	112.4	111.3	0.5	0.24
C	$m_{0a_1}^{3a_1}$	29 273.5	183.4	183.5	1.1	0.62
D	m_{1e}^{4e}	29 279.5	189.4	192.8	0.6	0.57
E	m_{1e}^{5e}	29 322.3	232.2	231.2	1.0	1.00
F	$m_{0a_1}^{6a_1}$	29 340.5	250.4	272.5	0.6	0.32

[a] Accuracy ± 2 cm^{-1}. [b] Accuracy ± 0.6 cm^{-1} for frequencies, ± 30% for relative intensities [c] Model used parameters: $V_3' = -268$ cm^{-1}, $V_6' = 50$ cm^{-1}, $F' = 4.5$ cm^{-1}, and $V_3'' = 200$ cm^{-1}, $V_6'' = 5$ cm^{-1}, $F''=4.6$ cm^{-1}. Intensities are scaled Franck−Condon factors.

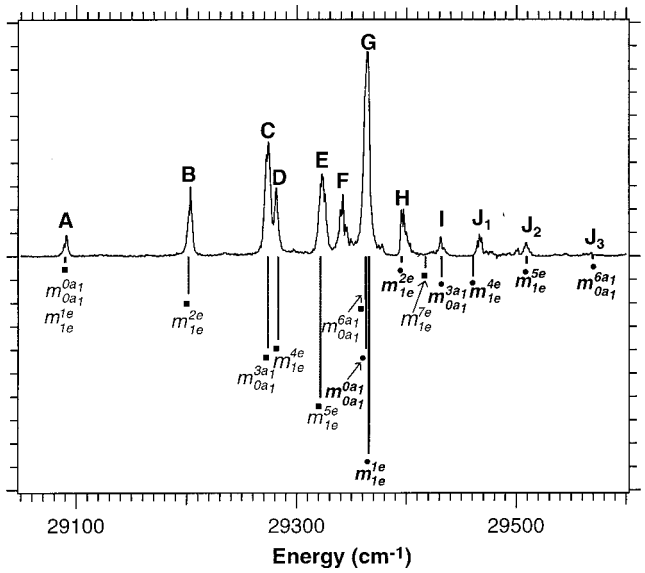

Figure 3. Expanded view of first torsional envelopes of the cis and *trans*-2-methylvinoxy radicals juxtaposed with stick representations of the fits to the 1-dimensional torsional model for the $\tilde{B}$ states of *cis*-2-methylvinoxy (squares) and *trans*-2-methylvinoxy (circles). Parameters of this fit in Tables 1 and 2. See text for details.

state barrier is frozen at 200 cm^{-1} with the sign of V_3'' opposite that of V_3' to produce the broad envelope of strong torsional transitions. The frequencies of the *A*−*B*−*C*−*D*−*E* bands of Figure 3 were optimized by searching a three-dimensional grid of values for the best F', V_3', and V_6' combination, as determined by the χ^2 parameter. The values of F' were constrained to the physically realistic range 4.5 to 6.0 cm^{-1}.[23,24] For *cis*-2-methylvinoxy, the resulting $\tilde{B}$-state torsional parameters are as follows: $V_3' = -268 \pm 20$ cm^{-1}, $V_6' = 50 \pm 20$ cm^{-1}, and $F' = 4.5 \pm 0.5$ cm^{-1}. This procedure is quite insensitive to the exact $\tilde{X}$-state values used in this fit ($V_3'' = 200$ cm^{-1}, $V_6'' = -5$ cm^{-1}, and $F'' = 4.6$ cm^{-1}), although these are in fact the values that will be extracted from fitting the hot bands of a warmer spectrum as described next.

A stick representation of this fit to the *A*−*B*−*C*−*D*−*E* series of bands is marked by the small squares in the expanded view of Figure 3. We believe the band *F*, whose torsional energy of 250 cm^{-1} lies very close to the $\tilde{B}$-state barrier, is likely a member of this *cis*-2-methylvinoxy torsional envelope despite the discrepancy with the fit. In previous work on the 1-methylvinoxy radical, whose methyl rotor torsional preference also changes on $\tilde{B} \leftarrow \tilde{X}$ excitation, we found that the fit to the simple one-dimensional model again broke down for vibronic bands at vibrational energies similar to the torsional barrier height.[9]

TABLE 2: *Trans*-2-methylvinoxy $\tilde{B}$-state Assignments

band	assign	energy[a] (cm^{-1})	$\tilde{B}$-state expt[b]	$\tilde{B}$-state calc[c]	intensity expt[b]	intensity calc[c]
G	$m_{0a_1}^{0a_1}, m_{1e}^{1e}$	29 363.1	0	0, 2.73	1.0	1.0
H	m_{1e}^{2e}	29 394.3	31.2	32.5	0.18	0.02
I	$m_{0a_1}^{3a_1}$	29 430.0	66.9	68.9	0.04	0.07
J_1	m_{1e}^{4e}	29 467.2	104.1	97.5	0.06	0.07
J_2	m_{1e}^{5e}	29 508.2	144.5	146.1	0.08	0.03
J_3	$m_{0a_1}^{7a_1}$	29 566.7	203.0	206.5	0.03	0.01

[a] Accuracy ± 2 cm^{-1}. [b] Accuracy ± 0.6 cm^{-1} for frequencies, ± 30% for relative intensities [c] Model used parameters: $V_3' = 60$ cm^{-1}, $V_6' = -30$ cm^{-1}, $F' = 5.5$ cm^{-1}, and $V_3'' = 330$ cm^{-1}, $V_6'' = 0$ cm^{-1}, $F'' = 5.5$ cm^{-1}. Intensities are scaled Franck−Condon factors.

The change in band shape that we see in band *F* versus the other bands in the series is also reminiscent of the $\tilde{B} \leftarrow \tilde{X}$ 1-methylvinoxy spectrum.

The additional stick spectrum in Figure 3 marked by the small circles shows our more *tentative* assignment of the torsional envelope of *trans*-2-methylvinoxy. As already mentioned, for *trans*-2-methylvinoxy theory predicts no change in the conformational preference of the methyl group upon excitation (Section V). Accordingly, we observe an intense origin band followed by a series of much less intense vibronic bands in the *G*−*H*−*I*−J_1−J_2 series. We label the bands this way to maintain consistency with our labels from a previous paper.[10]

Fitting this *G*−*H*−*I*−J_1−J_2 torsional envelope (Table 2) as described above for the *A*−*B*−*C*−*D*−*E* series of the cis isomer allows us to estimate experimental $\tilde{B}$-state torsional parameters for the trans isomer ($V_3' = 60 \pm 15$ cm^{-1}, $V_6' = -30 \pm 10$ cm^{-1}, and $F' = 5.5 \pm 0.5$). We resolve and assign no hot band data for this isomer, so the ground-state 3-fold barrier $V_3'' = 330$ cm^{-1} used in the fits was taken from the (3,3)-CAS+1+2/cc-pVDZ//(3,3)-CASSCF/cc-pVDZ ab initio calculations presented below. No $\tilde{X}$-state 6-fold barrier was included, and the rotational constant was set at the same value determined for the $\tilde{B}$-state. Once again, the calculated $\tilde{B} \leftarrow \tilde{X}$ spectrum is insensitive to the ground-state values if the ground-state barrier is larger than 100 cm^{-1}. As shown in Table 2, the frequency fit is good for five of the six bands, with J_1 the exception. The fit to intensities is less successful than that for *cis*-2-methylvinoxy or 1-methylvinoxy. Because we lack corroboration of these assignments from hot bands or from repetition of the torsional pattern for higher vibrational levels, we emphasize that we regard the *trans*-2-methylvinoxy assignments as tentative.

As mentioned, neither the cis nor the *trans*-2-methylvinoxy spectrum (Figure 1) exhibits the expected repetition of the torsional pattern. The bands labeled *K* and *M* occur at the vibrational energies 495 and 898 with respect to an origin at *G*. These values might correspond with the predicted frequencies for the C_1C_2O bend (534 cm^{-1}) and the C_1C_3 stretch (1189 cm^{-1}), but neither band exhibits the expected torsional pattern. The vibronic band *K* does have a series of bands following it that may appear to be a torsional pattern, but we have been unable to satisfactorily fit these bands to the torsional model. We leave the K and M bands as well as the nearby less intense bands unassigned.

B. Hot Bands. By adjusting the experimental conditions, we were able to collect warmer spectra of the mixture of cis- and *trans*-2-methylvinoxy radicals (Figure 4). In efficiently cooled spectra (Figures 2 and 3), the transitions arise predominantly from the $0a_1$ and $1e$ torsional levels in the ground state. In the warmer spectrum, we resolve bands arising from the higher

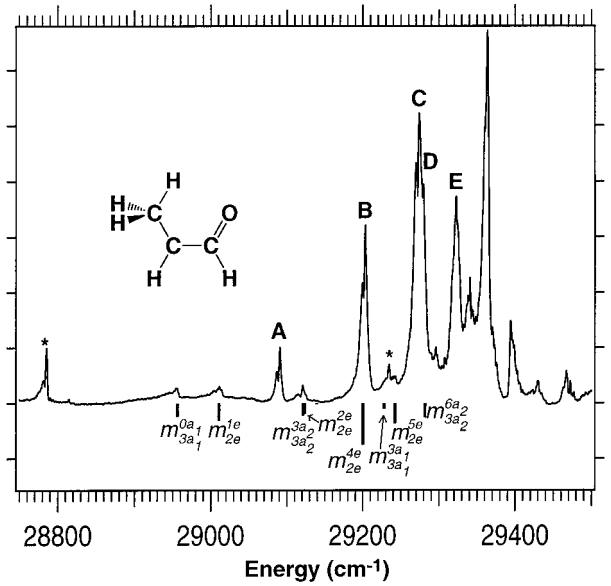

Figure 4. Expanded view of the first torsional envelope of a warmer $\tilde{B} \leftarrow \tilde{X}$ LIF spectrum than Figure 4. Stick spectrum and assignments below are based on a 1-dimensional torsional fit to the $\tilde{X}$-state of *cis*-2-methylvinoxy. Parameters of this fit in Table 3. The bands marked with the asterisks (*) are vinoxy transitions.

TABLE 3: *Cis*-2-methylvinoxy Hot Bands and Assignments

	energy (cm^{-1})		intensity	
assign	expt[a]	calc[b]	expt[a]	calc[b]
m_{2e}^{1e}	29 012	29 012	1	1
m_{2e}^{2e}	29 121	29 123	0.3	0.62
m_{2e}^{4e}		29 200		2.42
m_{2e}^{5e}	29 243	29 242	1.5	1.18
$m_{3a_2}^{3a_2}$	29 114	29 121	1	1
$m_{3a_2}^{6a_2}$		29 282		1.17
$m_{3a_1}^{0a_1}$	28 955	28 956	1	1
$m_{3a_1}^{3a_1}$	29 134	29 139	~0.02	0.09
$m_{3a_1}^{6a_1}$		29 228		0.42

[a] Energies measured at peak intensities accurate to ± 5 cm^{-1}. Intensities accurate to $\pm 30\%$. [b] Model parameters: $V_3' = -268$ cm^{-1}, $V_6' = 50$ cm^{-1}, $F' = 4.5$ cm^{-1}, and $V_3'' = 200$ cm^{-1}, $V_6'' = 5$ cm^{-1}, $F'' = 4.6$ cm^{-1}. Intensities are scaled Franck−Condon factors.

torsional levels $2e$, $3a_2$, and $3a_1$ in the ground state. The assigned hot bands all arise from the part of the spectrum attributed to *cis*-2-methylvinoxy radical. The fit to these bands gives the following $\tilde{B}$-state parameters: $V_3'' = 200 \pm 20$ cm^{-1}, $V_6'' = -5 \pm 10$ cm^{-1}, and $F'' = 4.6 \pm 0.5$ cm^{-1}. The $\tilde{B}$-state parameters used in the fit were $V_3' = -268$ cm^{-1}, $V_6' = 50$ cm^{-1}, and $F' = 4.5$ cm^{-1}, extracted from the $A-B-C-D-E$ series as explained in the previous section. Relative intensities of transitions arising from the same torsional state in the ground state are taken to be proportional to the model Franck−Condon factors. The intensity of the initial transition of each series is adjusted to match the experimental intensity to which it is being fit.

Table 3 shows the comparison between experimental $\tilde{X}$-state torsional frequencies and intensities and those from the fit. The model is quite successful in fitting both frequencies and intensities for the six hot bands that occur in sufficiently open regions of the spectrum to permit observation. Three other predicted bands would be blended with much stronger cold bands. The hot band spectrum not only provides information about the $\tilde{X}$ state, but also corroborates the $\tilde{B}$-state assignments, because the hot bands observed are consistent with the selection rules governing the $\tilde{B} \leftarrow \tilde{X}$ transitions between torsional states ($a_1 \leftarrow a_1$, $a_2 \leftarrow a_2$, $e \leftarrow e$).

TABLE 4: ab Initio Methyl Torsional Barriers (cm^{-1})[a] and Phases for $\tilde{B}$ and $\tilde{X}$-state cis and *trans*-2-methylvinoxy Radicals at Different Levels of Theory

method[b]	$\tilde{B}$-state	$\tilde{X}$-state
Cis-2-Methylvinoxy:		
experiment	-268 ± 20	200 ± 20
1 (5,4)-CAS/6-31G(d,p)d //**1d**	−138	178
2 (3,3)-CAS/cc-pVDZ[e]//**2e**	−124	206
3 (3,3)-CAS+1+2/cc-pVDZ[e]//**2e**	−106 (−101)[c]	239 (250)[c]
4 (3,3)-CAS+1+2/aug-cc-pVDZ[e]//**2e**	−207 (−209)[c]	164 (172)[c]
5 (3,3)-CAS+1+2/cc-pVTZ[e]//**2e**	−161 (−158)[c]	211 (222)[c]
6 QRHF-EOMEE-CCSD/cc-pVDZ[e]//**2e**	−83	232
7 QRHF-EOMEE-CCSD/ aug-cc-pVDZ[e]//**2e**	−198	
8 QRHF−CCSD(T)/cc-pVDZ[e]//**2e**		266
Trans-2-Methylvinoxy:		
experiment	60 ± 15	no data
1 (5,4)-CAS/6-31G(d,p)d //**1d**	−59 (*6-fold*)	266
2 (3,3)-CAS/cc-pVDZ[e]//**2e**	39	293
3 (3,3)-CAS+1+2/cc-pVDZ[e]//**2e**	91 (100)[c]	328 (335)[c]
4 (3,3)-CAS+1+2/aug-cc-pVDZ[e]//**2e**	67 (81)[c]	323 (334)[c]
5 (3,3)-CAS+1+2/cc-pVTZ[e]//**2e**	91 (106)[c]	341 (353)[c]
6 QRHF-EOMEE-CCSD/cc-pVDZ[e]//**6**	151	
8 QRHF-EOMEE-CCSD/ aug-cc-pVDZ[e]//**6**	156	

[a] All barriers are 3-fold (V_3) unless otherwise noted. *Positive* V_3 places the potential minimum with a methyl CH bond cis to the OC bond ($\alpha = 0$) and *negative* V_3 places the minimum with the CH bond trans to the OC bond. [b] The notation *X//Y* means geometry optimization was carried out using the level of theory *Y* and the energy at that geometry was evaluated using level of theory *X*. [c] Includes Davidson correction (refs 34 and 35). [d] Calculations done using Gaussian 98 (ref 28). [e] Calculations done using MOLPRO (refs 29−33).

V. ab Initio Calculations

A. Methods. In our recent paper, an extensive series of electronic structure methods were applied to the difficult problem of computing $\tilde{B}$ and $\tilde{X}$-state torsional barriers for the 1-methylvinoxy radical.[9] These included complete active space self-consistent field methods (CASSCF), multireference configuration interaction methods (CAS+1+2), and coupled-cluster methods (CC), each with a variety of basis sets. With the CASSCF method, the calculated 1-methylvinoxy $\tilde{B}$-state barrier height (193 cm^{-1}) fell significantly short of the experimentally determined value (751 cm^{-1}) regardless of basis set. A substantial discrepancy also existed between the calculated and experimental 1-methylvinoxy $\tilde{X}$-state torsional barrier heights (195 cm^{-1} vs 130 cm^{-1} respectively). The multireference CI calculations based on the CAS wave function as well as a variety of coupled-cluster calculations were better able to predict the torsional barrier for the 1-methylvinoxy species.

In the current theoretical study of 2-methylvinoxy radical (Table 4), we apply a subset of the same CASSCF, CAS+1+2, and coupled-cluster methods to both the $\tilde{B}$ and $\tilde{X}$ states. We summarize the methods here; additional details are given in the earlier work. [9] The bulk of the electronic structure calculations used three of the Dunning correlation-consistent basis sets, the double-ζ (cc-pVDZ), the augmented double-ζ (aug-cc-pVDZ) and the triple-ζ (cc-pVTZ) basis sets.[25−27] The exceptions are the GAUSSIAN 98[28] CASSCF calculations, which used the 6-31G** basis set. The CAS calculations used the program packages MOLPRO and GAUSSIAN. The coupled-cluster

calculations used the version of the ACES II program system[29] maintained by Stanton and Gauss.

As before, three different reference wave functions were considered in the multireference calculations. The majority of the calculations employ a three-electron, three-orbital CAS reference wave function. The three active orbitals are the singly occupied radical orbital (3a") and the CO π and π^* orbitals (2a" and 4a"). For the $\tilde{B}$ state, this reference wave function is workable only for geometries of C_s symmetry. For geometries of C_1 symmetry one needs to enlarge the reference space to include the oxygen lone pair a′ orbital. The (5,4) calculations listed in the Table 4 and described later in this section use this active space including the oxygen lone pair a′ orbital and its two electrons. Using these reference configurations, internally contracted, multireference, singles and doubles configuration interaction calculations (CAS+1+2) were carried out using the MOLPRO program.[30−34] The effects of higher order excitations (beyond singles and doubles) were examined using multireference Davidson corrections.[35,36]

In the 1-methylvinoxy work,[9] we explored several different approaches based on the coupled cluster (CC) approximation. On the basis of that work, we choose to apply the equation-of-motion coupled-cluster method for excited states (EOMEE-CC)[37] to the 2-methyvinoxy radicals. The reference determinant is again obtained from the quasi-restricted Hartree−Fock method of Rittby and Bartlett.[38] For the 2-methylvinoxies, the ground state determinant is that with the $1a''^2\ 2a''^2\ 3a''^1\ 4a''^0$ occupation of a″ orbitals; both of the important configurations for the $\tilde{B}$ state are related to this determinant by a single excitation. Hence, EOMEE-CC offers a balanced treatment of the important configurations that describe the $\tilde{B}$ state that is not possible to achieve with the usual single reference CC methods using any choice of orbitals. The resulting calculations are called QRHF/EOMEE-CCSD.

In all cases, the 3-fold potential parameter V_3 is estimated as the difference in energy between the conformation with $\alpha = 0°$ and the conformation with $\alpha = 180°$. Because geometry optimizations relaxed all other geometric parameters at $\alpha = 0°$ and 180°, we call these estimates the vibrationally adiabatic torsional barrier. Zero-point corrections to the vibrationally adiabatic barrier were applied at those levels of theory for which the geometry was optimized at both $\alpha = 0°$ and 180°. They were always small, 2−15 cm^{-1} in both the $\tilde{X}$ and $\tilde{B}$ states.

B. Results. The CASSCF calculations indicate that the energies of *cis*- and *trans*-2-methylvinoxy are similar in both the $\tilde{X}$ and $\tilde{B}$ states and that a substantial barrier to *cis*−*trans* isomerization exists in both electronic states. For example, the CASSCF(5,4)/6-31G** level of theory finds cis below trans by 0.5 kcal/mol in the $\tilde{X}$state and by 0.6 kcal/mol in the $\tilde{B}$ state. The calculated isomerization barrier viewed from the cis →trans direction is 10.0 kcal/mol in the $\tilde{X}$ state and 8.2 kcal/mol in the $\tilde{B}$ state. This justifies our treatment of the spectrum as arising from two noninteracting isomers in both electronic states. Although not the focus of our study, the adiabatic electronic excitation energy is 29 595 cm^{-1} (cis) and 29 626 cm^{-1} (trans) at the (3,3)-CAS+1+2/cc-pVDZ level of theory. Both these values are in good agreement with the experimental values of 29 090 and 29 363 cm^{-1} respectively.

The 3-fold potential parameters V_3 determined by various theoretical methods are compiled in Table 4 for both the cis and trans isomers in both the $\tilde{X}$ and $\tilde{B}$ electronic states. The notation in Table 4 follows the usual convention of listing the method of calculation to the left of the double-slash and the method with which the geometry was optimized to the right. For the $\tilde{B}$ state of *cis*-2-methylvinoxy, the various methods give V_3' values that range from −209 cm^{-1} to −83 cm^{-1}, compared to the experimental estimate of −268 ± 30 cm^{-1}. For the $\tilde{X}$ state of the cis isomer, the calculated barriers range from +266 cm^{-1} to +164 cm^{-1}, compared to the experimental value of +200 ± 30 cm^{-1}. Recall that theory was used to fix the signs of V_3' and V_3'', but theory and experiment agree that the sign must change from $\tilde{X}$ to $\tilde{B}$.

For the $\tilde{B}$ state of *trans*-2-methylvinoxy, the calculated values of V_3'' range from +198 cm^{-1} to +39 cm^{-1}, compared to +60 ± 15 cm^{-1} determined by experiment. Again, agreement of the sign is not significant. For the $\tilde{X}$ state of *trans*-2-methylvinoxy, the calculated values range from 353 to 266 cm^{-1}. No experimental methyl torsional barrier was determined.

As might be expected, the ground state methyl torsional barriers are generally less sensitive to theoretical method and basis set than the excited-state torsional barriers. For the $\tilde{B}$ state of *cis*-2-methylvinoxy, whose experimental barrier is quite firmly established, all methods substantially underestimate the barrier height. Agreement between experiment and theory is comparable for the multireference CAS and coupled-cluster methods. For the $\tilde{B}$ state of *trans*-2-methylvinoxy, whose experimental barrier is more tentative, the multireference CAS methods agree with experiment better than the coupled cluster methods. However, the relative strengths of the various methods cannot truly be assessed without additional investigation of basis set effects.

VI. Discussion

A. Missing Bands in $\tilde{B} \leftarrow \tilde{X}$ LIF Spectra. In the unsubstituted vinoxy radical, the increase in the quantum yield of CH_3 and CO photofragments coincides with the fairly monotonic shortening of the $\tilde{B}$-state fluorescence lifetime.[39] Both experimental and theoretical studies on vinoxy indicate that out-of-plane modes are most effective in promoting photochemistry.[11,39,40] In both the 1-methylvinoxy and the 2-methylvinoxy spectra, we observe shorter lifetimes toward higher energy among those states discernible by LIF.[10] However, in the LIF spectrum of the mixture of the 2-methylvinoxy isomers, the absence of regular, assignable structure above 29 500 cm^{-1} would seem to indicate that *many* states at low vibrational energy have very small fluorescence quantum yields. Evidently a very few states above 29 500 cm^{-1} are relatively impervious to photochemical decay, e.g., bands K,L, and M in Figure 2. The identity of those states that do appear then becomes quite interesting, but we cannot assign them here.

B. Methyl Torsional Potential. In previous studies of internal methyl rotation in substituted toluenes, it was found that both the magnitude of the barrier to internal rotation and the conformational preference of the methyl group depend sensitively on the electronic structure of the molecule.[20,22,41] We found a strong correlation between torsional barrier height and the difference in bond order of the two ring CC bonds vicinal to the methyl CH bonds. In all cases, the methyl prefers the conformation that places one CH bond in the plane of the frame cis to the vicinal bond of higher bond order. This is consistent with the methyl conformational preferences of other molecules such as acetone and 2-methylpropene in which the methyl group is attached to an sp^2 hybridized carbon. Steric effects are also important for *ortho*-substituted species. For instance, the methyl torsional barrier in *ortho*-chlorotoluene is significantly larger than in *meta*-chlorotoluene (481 cm^{-1} vs 2 cm^{-1}).

For the unsubstituted vinoxy species, it has been demonstrated both experimentally[42,43] and theoretically[40,44] that the $\tilde{B} \leftarrow \tilde{X}$

TABLE 5: Comparison of Calculated Geometries for the Methylvinoxy Isomers[a]

	X̃-state			B̃-state		
	c-2-mv	t-2-mv	1-mv	c-2-mv	t-2-mv	1-mv
$r(C_2O)$	1.223	1.224	1.221	1.365	1.363	1.362
$r(C_1C_2)$	1.438	1.434	1.451	1.450	1.453	1.451
$r(C_3C_1)/r(C_3C_2)$[b]	1.495	1.495	1.514	1.496	1.497	1.493
$\angle OC_2C_1$	123.5	122.9	120.2	121.7	121.4	120.1
$\angle C_2C_1C_3/C_1C_2C_3$[c]	123.0	123.6	118.0	121.3	121.0	122.6

[a] Geometries calculated using (5,4)-CASSCF/6-31G** (All distances in Angstroms and angles in degrees). [b] The bond length $r(C_3C_1)$ is for the cis and *trans*-2-methylvinoxy radicals and $r(C_3C_2)$ for the 1-methylvinoxy radical. [c] The bond angle $\angle C_2C_1C_3$ is for the cis and *trans*-2-methylvinoxy radicals and $\angle C_1C_2C_3$ for the 1-methylvinoxy radical.

electronic excitation, a $\pi^* \leftarrow \pi$ transition, results in a dramatic lengthening in the CO bond. Not surprisingly, computational work predicts that this lengthening of the CO bond from about 1.22 Å to 1.36 Å also occurs in each of the three methylvinoxy isomers (Table 5). In the 1-methylvinoxy radical, the CO bond is vicinal to the methyl group CH bonds, but in the 2-methylvinoxy radicals it is not. In the case of the *cis*-2-methylvinoxy radical, the CO bond bears the same relationship to the methyl group as an *ortho*-substituent in the substituted toluenes, so we might expect it to affect the torsional barrier by a steric effect. In contrast, the *trans*-2-methylvinoxy methyl group lies far from the CO bond, and it is unlikely that there is any direct interaction between them.

The behavior of the methyl torsional potential in *trans*-2-methylvinoxy is qualitatively consistent with the substituted toluenes and with 2-methylpropene. The C_1C_2 and the C_1H bonds are vicinal to the CH bonds of the methyl group. The C_1C_2 bond has significant double bond character in both the X̃ and B̃ states; accordingly, the calculations predict that the preferred conformation in both states places one methyl CH bond cis to the C_1C_2 bond. The most extensive calculations also predict that the 3-fold torsional barrier decreases from 341 cm^{-1} in the X̃-state to 91 cm^{-1} in the B̃ state (Table 4). This is qualitatively consistent with the fact that the C_1C_2 bond lengthens upon excitation by approximately 0.02 Å (Table 5) and thus loses some of its double bond character, but the magnitude of the change suggests other factors as well. We return to this point below.

The *cis*-2-methylvinoxy methyl behavior is less readily interpreted. Now the two bonds vicinal to the methyl CH bonds are the C_1H single bond and the C_1C_2 bond. The methyl group changes its preferred conformation upon electronic excitation, with one CH bond of methyl cis to C_1C_2 in the X̃ state but with one CH bond of methyl trans to C_1C_2 in the B̃ state. Three competing effects may influence the methyl potential in *cis*-2-methylvinoxy. According to the (5,4)-CASSCF/6-31G** calculations, the C_1C_2 bond length of 1.438 Å in the cis isomer lengthens upon excitation by only 0.01 Å (Table 5). In both the X̃ and B̃ states of *cis*-2-methylvinoxy, the C_1C_2 bond has significant double bond character, which favors the methyl conformation with one CH bond cis to the C_1C_2 bond as occurs in the X̃ state. The oxygen atom's lone pair in the molecular plane should cause steric repulsion with the CH bonds of methyl. By analogy to the effect of an *ortho* substituent in the substituted toluenes, this should favor the methyl conformation with one CH bond trans to the C_1C_2 bond as occurs in the B̃ state. However, these factors are present in both the X̃ and B̃ states of cis-2-methylvinoxy. The slight lengthening of the C_1C_2 bond on electronic excitation goes in the right direction to favor the trans methyl conformer, but is too small to explain the magnitude of the potential change. The substantial lengthening of the CO bond on electronic excitation goes in the wrong direction, presumably *diminishing* steric repulsion and thus favoring the cis methyl conformation in the B̃ state, opposite to the observed result.

Hence, we seek a third qualitative contribution to the methyl barrier that provides the strong shift in preference from cis to trans conformation on electronic excitation. To a first approximation, the $\pi^* \leftarrow \pi$ electronic transition breaks the CO π-bond, leaving one electron in the π_{CO} bond, which is polarized toward the oxygen atom, while promoting one electron to the π^*_{CO} bond, which is polarized toward the C_2 atom. A third unpaired electron remains localized in the out-of-plane p orbital on the C_2 atom. The B̃-state vinoxy radicals thus have a doublet-coupled, *tri-radical* character.

We believe that the half-filled π^*_{CO} orbital with its large amplitude on C_2 provides an excellent electron *acceptor* that interacts most favorably with the methyl σ_{CH} bonds in the trans configuration favored in the B̃ state. With this in mind, UHF/6-311++G** ab initio calculations were performed on singlet (**1**) and triplet (**2**) propene; the latter was constrained to have a planar molecular frame to mimic that of *cis*-2-methylvinoxy.

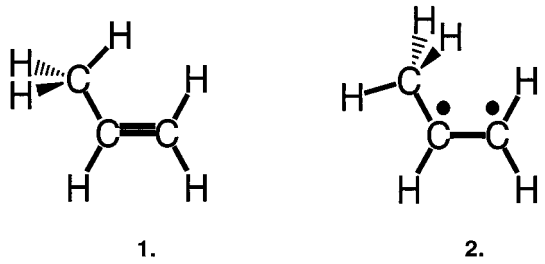

1. **2.**

As expected, in singlet propene the methyl group prefers the conformation shown, with one methyl CH bond cis to the vicinal CC double bond and a large torsional barrier ($V_3 = +724$ cm^{-1}). In the triplet propene, the preferred conformation places one methyl CH bond trans to the vicinal CC *single* bond; the torsional barrier reverses but remains substantial ($V_3 = -463$ cm^{-1}).

These results corroborate the suggestion that the $\pi^* \leftarrow \pi$ excitation in both 2-methylvinoxy radicals substantially affects the methyl torsional potential in the direction favoring one methyl CH bond trans to the C_1C_2 bond. For *cis*-2-methylvinoxy in both the X̃ and B̃ states, a competition exists between the C_1C_2 double bond character (favoring a methyl CH bond cis to that C_1C_2 bond) and the steric effect of the oxygen atom (favoring a methyl CH bond trans to the C_1C_2 bond). Based on the X̃-state result, the C_1C_2 double bond character is the stronger effect. However, in the B̃-state, the $\pi^* \leftarrow \pi$ excitation generates significant radical character on C_2, which produces a third contribution to the methyl rotor barrier that strongly favors the trans methyl conformation.

Returning to the B̃ state of the *trans*-2-methylvinoxy radical, we expect this same $\pi^* \leftarrow \pi$ effect again to favor the trans methyl conformation. Now the steric effect from oxygen is absent, but the C_1C_2 double bond character favoring the cis methyl conformation remains intact in both X̃ and B̃ states. Accordingly, the most extensive calculations result in a substantial X̃-state barrier (calculated $V_3 = +341$ cm^{-1}) in favor of the cis methyl conformation. The B̃-state barrier is substantially attenuated (calculated $V_3 = +91$ cm^{-1} in reasonable agreement with the experimental result of $+60$ cm^{-1}) but the cis methyl conformation is still mildly favored. The influence of π radical character on C_2 evidently lowers the barrier to

internal methyl rotation but is not strong enough to change the conformational preference by itself.

In summary, the data and calculated geometries seem qualitatively consistent with the existence of three factors contributing to the methyl rotor barrier in *cis*-2-methylvinoxy: C_1C_2 double bond character, favoring the cis conformation of the methyl group in both $\tilde{X}$ and $\tilde{B}$ states; steric repulsion by the in-plane lone pair of the oxygen atom, favoring the trans conformation in both $\tilde{X}$ and $\tilde{B}$ states; and π radical character on C_2 in the $\tilde{B}$ state only, favoring the trans conformation. In *trans*-2-methylvinoxy, the steric effect from oxygen is absent. Although these qualitative arguments are appealing, it is not easy to assign quantitative contributions to each effect and to test for additivity of effects.

VII. Conclusions

The predictions of methyl group conformational preferences by electronic structure theory have been very helpful in assigning the $\tilde{B} \leftarrow \tilde{X}$ LIF spectrum of the mixture of cis and *trans*-2-methylvinoxy radicals. The calculated geometries have also been useful in understanding the methyl torsional potentials for these species. However, as for the 1-methylvinoxy radical,[9] theory continues to have difficulty predicting the methyl torsional barrier heights to high accuracy, especially in the $\tilde{B}$ state.

Acknowledgment. J.C.W. and L.B.H. thank the Department of Energy, Office of Basic Energy Sciences, Division of Chemical Sciences for generous support of this work (Grant No. DE-FG02-92ER14306 and Contract No. W-31-109-Eng-38, respectively). J.C.W. and J.F.S. thank the National Science Foundation (CHE00-71458 and CHE98-73818, respectively) for support. J.F.S. also acknowledges support from the Robert A. Welch Foundation. J.C.W. and S.W. acknowledge many helpful discussions with Prof. Frank Weinhold.

References and Notes

(1) Cvetonic, R. J.; Singleton, D. L. *Rev. Chem. Int.* **1984**, *5*, 183.
(2) Schmoltner, A. M.; Chu, P. M.; Brudzynski, R. J.; Lee, Y. T. *J. Chem. Phys.* **1989**, *91*, 6926.
(3) Quandt, R.; Min, Z.; Wang, X.; Bersohn, R. *J. Phys. Chem. A* **1998**, *102*, 60.
(4) Niki, H.; Maker, P. D.; Savage, C. M.; Breitenbach, L. P.; Hurley, M. D. *J. Phys. Chem.* **1987**, *91*, 941.
(5) Parmenter, C. S. *J. Phys. Chem.* **1982**, *86*, 1735.
(6) Moss, D. B.; Parmenter, C. S.; Ewing, G. E. *J. Chem. Phys.* **1987**, *86*, 51.
(7) Moss, D. B.; Parmenter, C. S. *J. Chem. Phys.* **1993**, *98*, 6897.
(8) Timbers, P. J.; Parmenter, C. S.; Moss, D. B. *J. Chem. Phys.* **1994**, *100*, 1028.
(9) Williams, S.; Harding, L. B.; Stanton, J. F.; Weisshaar, J. C. *J. Phys. Chem. A* (in press) **2000**.
(10) Williams, S.; Zingher, E.; Weisshaar, J. C. *J. Phys. Chem. A* **1998**, *102*, 2297−2301.
(11) Brock, L. R.; Rohlfing, E. A. *J. Chem. Phys.* **1997**, *106*, 10 048.
(12) Washida, N.; Inomata, S.; Furubayashi, M. *J. Phys. Chem. A* **1998**, *102*, 7924−7930.
(13) Furubayashi, M.; Bridier, I.; Inomata, S.; Washida, N.; Yamashita, K. *J. Chem. Phys.* **1997**, *106*, 6302−6309.
(14) Bunker, P. R. *Molecular Symmetry and Spectroscopy*; Academic: New York, 1979.
(15) Longuet-Higgins, H. C. *Mol. Phys.* **1963**, *6*, 445.
(16) Walker, R. A.; Richard, E. C.; Lu, K.-T.; Weisshaar, J. C. *J. Phys. Chem.* **1995**, *99*, 12 422.
(17) Lu, K.-T.; Weisshaar, J. C. *J. Chem. Phys.* **1993**, *99*, 4247.
(18) Lu, K.-T.; Eiden, G. C.; Weisshaar, J. C. *J. Phys. Chem.* **1992**, *96*, 9742.
(19) Lin, C. C.; Swalen, J. D. *Rev. Mod. Phys.* **1959**, *31*, 841.
(20) Richard, E. C.; Walker, R. A.; Weisshaar, J. C. *J. Chem. Phys.* **1995**, *104*, 4451.
(21) Barnhard, K. I.; He, M.; Weiner, B. R. *J. Phys. Chem.* **1996**, *100*, 2784−2790.
(22) Feldgus, S. H.; Schroeder, M. J.; Walker, R. A.; Woo, W.-K.; Weisshaar, J. C. *Int. J. Mass Spec. Ion Proc.* **1996**, *159*, 231.
(23) Zhao, Z.-Q.; Parmenter, C. S.; Moss, D. B.; Bradley, A. J.; Knight, A. E. W.; Owens, K. G. *J. Chem. Phys.* **1992**, *96*, 6362.
(24) Ikoma, H.; Takazawa, K.; Emura, Y.; Ikeda, S.; Abe, H.; Hayashi, H.; Fujii, M. *J. Chem. Phys.* **1996**, *105*, 10 201.
(25) Dunning, T. H., Jr. *J. Chem. Phys.* **1989**, *90*, 1007.
(26) Kendall, R. A.; Dunning, T. H., Jr. *J. Chem. Phys.* **1992**, *96*, 6796.
(27) Woon, D. E.; Dunning, T. H., Jr. *J. Chem. Phys.* **1993**, *98*, 1358.
(28) Gaussian 98 (Revision A.6), M. J. F., G. W. Trucks, H. B. Schlegel, G. E. Scuseria, M. A. Robb, J. R. Cheeseman, V. G. Zakrzewski, J. A. Montgomery, R. E. Stratmann, J. C. Burant, S. Dapprich, J. M. Millam, A. D. Daniels, K. N. Kudin, M. C. Strain, O. Farkas, J. Tomasi, V. Barone, M. Cossi, R. Gaussian 98 (Revision A.6), M. J. Frisch, G. W. Trucks, H. B. Schlegel, G. E. Scuseria, M. A. Robb, J. R. Cheeseman, V. G. Zakrzewski, J. A. Montgomery, R. E. Stratmann, J. C. Burant, S. Dapprich, J. M. Millam, A. D. Daniels, K. N. Kudin, M. C. Strain, O. Farkas, J. Tomasi, V. Barone, M. Cossi, R. Cammi, B. Mennucci, C. Pomelli, C. Adamo, S. Clifford, J. Ochterski, G. A. Petersson, P. Y. Ayala, Q. Cui, K. Morokuma, D. K. Malick, A. D. Rabuck, K. Raghavachari, J. B. Foresman, J. Cioslowski, J. V. Ortiz, B. B. Stefanov, G. Liu, A. Liashenko, P. Piskorz, I. Komaromi, R. Gomperts, R. L. Martin, D. J. Fox, T. Keith, M. A. Al-Laham, C. Y. Peng, A. Nanayakkara, C. Gonzalez, M. Challacombe, P. M. W. Gill, B. G. Johnson, W. Chen, M. W. Wong, J. L. Andres, M. Head-Gordon, E. S. Replogle and J. A. Pople, Gaussian, Inc., Pittsburgh, PA, 1998.
(29) Stanton, J. F.; Gauss, J.; Watts, J. D.; Lauderdale, W. J.; Bartlett, R. J. *Int. J. Quantum Chem. (Symposium)* **1993**, *26*, 879.
(30) MOLPRO is a package of ab initio programs written by Werner, H.-J. a. K., P. J. with contributions from Almlof, J., Amos, R. D., Berning, A., Cooper, D. L., Deegan, M. J. O., Dobbyn, A. J., Eckert, F., Elbert, S. T., Hampel, C., Lindh, R., Lloyd, A. W., Meyer, W., Nicklass, A., Peterson, K., Pitzer, R., Stone, A. J., Taylor, P. MOLPRO is a package of ab initio programs written by Werner, H.-J. and Knowles, P. J. with contributions from Almlof, J., Amos, R. D., Berning, A., Cooper, D. L., Deegan, M. J. O., Dobbyn, A. J., Eckert, F., Elbert, S. T., Hampel, C., Lindh, R., Lloyd, A. W., Meyer, W., Nicklass, A., Peterson, K., Pitzer, R., Stone, A. J., Taylor, P. R., Mura, M. E., Pulay, P., Schutz, M., Stoll, H., Thorsteinsson, T.
(31) Werner, H.-J.; Knowles, P. J. *J. Chem. Phys.* **1988**, *89*, 5803.
(32) Knowles, P. J.; Werner, H.-J. *Chem. Phys. Lett.* **1988**, *145*, 514.
(33) Knowles, P. J.; Werner, H.-J. *Chem. Phys. Lett.* **1985**, *115*, 259.
(34) Werner, H.-J.; Knowles, P. J. *J. Chem. Phys.* **1985**, *82*, 5053.
(35) Langkoff, S. R.; Davidson, E. R. *Int. J. Quantum Chem.* **1974**, *8*, 61.
(36) Silver, D. W.; Davidson, E. R. *Chem. Phys. Lett.* **1978**, *52*, 403.
(37) Stanton, J. F.; Bartlett, R. J. *J. Chem. Phys.* **1993**, *98*, 7029.
(38) Rittby, M.; Bartlett, R. J. *J. Phys. Chem.* **1988**, *92*, 3033.
(39) Osborn, D. L.; Choi, H.; Mordaunt, D. H.; Bise, R. T.; Neumark, D. M.; Rohlfing, C. M. *J. Chem. Phys.* **1997**, *106*, 3049.
(40) Yamaguchi, M. *Chem. Phys. Lett.* **1994**, *221*, 531−536.
(41) Lu, K.-T.; Weinhold, F.; Weisshaar, J. C. *J. Chem. Phys.* **1995**, *102*, 6787.
(42) DiMauro, L. F.; Heaven, M.; Miller, T. A. *J. Chem. Phys.* **1984**, *81*, 2339−2346.
(43) Endo, Y.; Saito, S.; Hirota, E. *J. Chem. Phys.* **1985**, *83*, 2026.
(44) Dupuis, M.; Wendoloski, J. J.; Lester, J. W. A. *J. Chem. Phys.* **1981**, *76*, 488.